

Using Fuzzy Systems to Infer Memory Impairment from MRI

Yo-Ping Huang^{1,2}, Samuele M.M. Zaza¹, Wen-Jang Chu³, Robert Krikorian³, Frode Eika Sandnes^{4,5}

¹Department of Electrical Engineering
National Taipei University of Technology
Taipei, Taiwan 10608

e-mail: yphuang@ntut.edu.tw; zaza.samuele@gmail.com

²Department of Computer Science and Information Engineering
National Taipei University
New Taipei City, Taiwan 23741

³Department of Psychiatry and Behavioral Neuroscience
University of Cincinnati
Cincinnati, Ohio 45229 U.S.A.

e-mail: wen-jang.chu@uc.edu; krikorr@ucmail.uc.edu

⁴Faculty of Technology, Art and Design
Oslo and Akershus University College of Applied Sciences
Oslo, Norway

Email: Frode-Eika.Sandnes@hioa.no

⁵Faculty of Technology
Westerdals School of Art, Communication and Technology
Oslo, Norway

Abstract—Alzheimer’s Disease (AD) is a common form of dementia which mostly affects elderly people. Gradual loss in memory and declining cognitive functions are core symptoms associated with AD. Conventional brain images do not provide sufficient information to diagnose AD at an early stage. To delay the progression of memory impairment there is a dire need to develop systems capable of early AD diagnosis. This paper describes a proposed fuzzy method for inferring the risk of dementia using the brain cortical thickness and hippocampus thickness. The aim is to develop a reliable index that allows the evaluation of brain health. The dementia index poses potential to become a biologically-based biomarker for the clinical assessment of patient’s dementia. Results show that the inference value of patient with mild cognitive impairment (MCI) is significantly higher than that of healthy (Control) or schizophrenia (SCZ) patients. Our results suggest that a higher inference value indicates that the patient is at higher risk and is more likely to eventually progress to AD. The system was also tested with age-associated memory impairment (AAMI) patients. The results confirm that our model is able to distinguish between these four patient groups.

Keywords: AD, brain cortex, dementia risk, fuzzy system, MRI.

1. INTRODUCTION

According to Alzheimer's Disease International (ADI), there were an estimated 44.4 million people with dementia worldwide in 2013 which is projected to increase to 75.6 million in 2030, and 135.5 million in 2050. Moreover, with 7.7 million new cases of dementia every year, there is one new case diagnosed every 4 seconds [1]. Developed countries are impacted the most because of their aging population. The cost of healthcare associated with dementia is estimated to be \$604 million a year worldwide, and this cost is mostly driven by late AD diagnosis. Several attempts have been made to develop early AD diagnosis systems.

Dickerson et al. [2-3] biologically marked brain amyloid- β amino acids and classified the markers into high, medium and low risk of AD symptoms. Among the 159 participants in the study, 19 were classified as high risk, 116 as medium risk and 24 as low risk. After three years of observation on participant variation, 21.4% of the high risk group had reduced cognition, 6.6% for medium risk group and 0% for low risk group. This study verified that the variation of cortical thickness is highly correlated to the risk that progresses to AD.

Chung et al. [4-5] described a framework to determine the brain cortical thickness from MRI and further determined the cortical thickness distribution characteristics using signal processing methods.

This study improved upon Chung et al.'s approach [4-5] by the introduction of fuzzy logic. Moreover, this work extends previous studies on the correlation between cortical thickness and dementia status [6,7] by introducing the hippocampus volume as a parameter into the model to enhance the prediction accuracy. Brain atrophy is a common biological process associated with AD and normal aging brains. The hippocampal atrophy and thinner cortical cortex are common neuroimaging characteristics in both populations. Thus, we approach our study using fuzzy logic since hard true and false boundaries cannot always be defined [15].

This paper is organized as follows. In section 2 a brief introduction of the software used for analysis is described. Section 3 explains the processes of 3D image reconstruction. In Section 4 the detailed fuzzy modeling is presented to infer the dementia risk. Experimental results and their analyses are described in Section 5. Conclusions are made in Section 6.

2. METHODS

The first step in our system consists of constructing the 3D model of the patients' brains using FreeSurfer (<http://surfer.nmr.mgh.harvard.edu/>), an open source application developed by Harvard University that takes T1-

weighted MRI as input. First, it is decided if a single brain hemisphere is to be analyzed or whether to analyze the entire brain. Next, heat kernel smoothing is used to simulate the heat transmission and subsequently to remove noise. Third, the spherical brain image is used to reconstruct the distribution of the cortical thickness which again is converted into a 2D map. Finally, the min-max diagram method [8] is used to match the homology of cortical thickness and plot its topological characteristics. The goal is to identify at-risk patients. Therefore, images in this study included MCI (a high-risk group that has progressed into AD), AAMI (a low-risk group that exhibits the same memory loss and declining cognitive function as the MCI group), SCZ (a psychiatric disorder group with memory deficit and cognitive dysfunction) and a control group.

Both unilateral hippocampus volumes were analyzed using FreeSurfer. Data such as the number of voxels and volume of brain sub-regions are provided by FreeSurfer. An example of such statistics is illustrated in Fig. 1, which displays the volume of each unilateral hippocampus (in mm^3) and other brain sub-regions such as the hippocampus volume and the total intracranial volume (TIV). TIV is a reference used to normalize and compare the volumes among the different patients while reconstructing the brain model. Though the hippocampus is present in both the brain hemispheres, the input of our fuzzy system is a single hippocampus seen as the summation of the left and right volumes.

The input to the proposed fuzzy system is the matching homology of birth and death from cortical thickness, either of the overall brain or unilateral hemisphere. By projecting the centroids of the fuzzy clusters onto the birth-axis and death-axis we are able to draw the corresponding membership functions and the fuzzy rules of the system.

Figure 2 illustrates the processing steps involved. The third input membership functions are designed differently for hippocampus step. By ordering the normalized hippocampus volumes of all the patients, they are constructed using the highest, medium and smallest volumes. The normalized volumes are scaled by a factor of 10^3 due to their small magnitude.

Ethics Statement: Written informed consent was obtained from all participants. This study was approved by the Institutional Review Board of the University of Cincinnati (IRB 09-04-16-01EE). The research was conducted according to the principles of the Declaration of Helsinki. A detailed personal history, general health examination, and lifestyle questionnaire were conducted with all participants.

#	ColHeaders	Index	SegId	NVoxels	Volume_mm3	StructName	normMea
1	4	19533	19533.2			Left-Lateral-Ventricle	
2	5	463	462.6			Left-Inf-Lat-Vent	
3	7	17964	17963.7			Left-Cerebellum-White-Matter	
4	8	52173	52172.6			Left-Cerebellum-Cortex	
5	10	6553	6553.0			Left-Thalamus-Proper	
6	11	3514	3513.8			Left-Caudate	
7	12	5789	5789.4			Left-Putamen	
8	13	1841	1841.1			Left-Pallidum	
9	14	673	673.2			3rd-Ventricle	
10	15	1343	1343.3			4th-Ventricle	
11	16	20943	20943.0			Brain-Stem	
12	17	4104	4104.4			Left-Hippocampus	
13	18	1287	1286.8			Left-Amygdala	
14	24	1011	1011.0			CSF	
15	26	453	453.4			Left-Accumbens-area	
16	28	3937	3936.8			Left-VentralDC	
17	30	72	71.7			Left-vessel	
18	31	1327	1327.3			Left-choroid-plexus	
19	43	21782	21782.0			Right-Lateral-Ventricle	
20	44	415	415.3			Right-Inf-Lat-Vent	
21	46	14617	14617.1			Right-Cerebellum-White-Matter	
22	47	53726	53726.2			Right-Cerebellum-Cortex	
23	49	6126	6125.7			Right-Thalamus-Proper	
24	50	3559	3559.5			Right-Caudate	
25	51	5955	5954.9			Right-Putamen	
26	52	1521	1520.7			Right-Pallidum	
27	53	3700	3700.0			Right-Hippocampus	
28	54	1666	1665.8			Right-Amygdala	
29	58	444	444.3			Right-Accumbens-area	
30	60	3986	3986.1			Right-VentralDC	

Fig. 1. File aseg.stats. Rows 12 and 27 show the left and right hippocampus volumes, respectively.

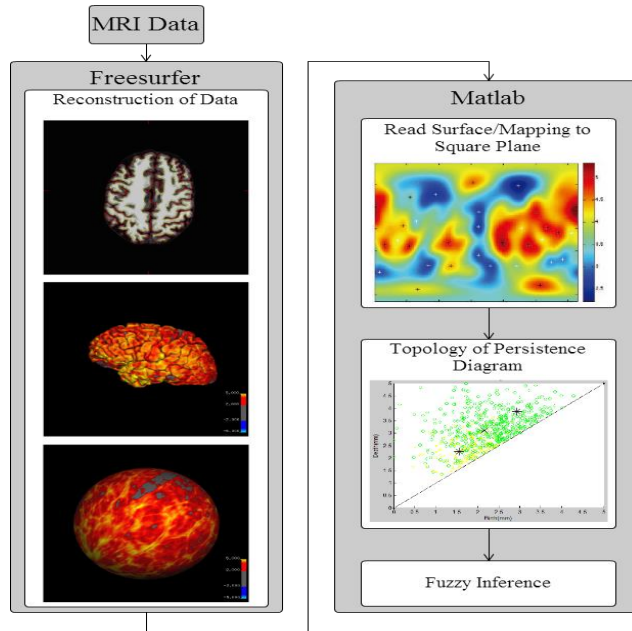


Fig. 2. The steps of the proposed method to infer the risk of AD.

3. DATA PREPARATION

This section describes the steps needed to prepare the input to the fuzzy system.

3.1 3D Brain Reconstruction

The first step consists of making a 3D model of the patient's brain, retrieving the information about the hippocampus volumes and to normalize the volumes using the intracranial volume. Given MRI images of the

patient's brain, FreeSurfer is capable of performing several operations, including cortical surface reconstruction, cortical segmentation, cortical thickness estimation and subregions volume estimation. The tools in the suite construct models of the boundary between white matter and cortical gray matter as well as the pial surface by going through several stages [10] while registering the volume according to a Talaraich atlas. Once these surfaces are known, an array of anatomical measures can be acquired, including cortical thickness, surface area, curvature, and surface normal at each point on the cortex. The processing procedures for the creation of cortical models require good quality T1 weighted MRI data, such as a Siemens MPRAGE (examples of appropriate Siemens scanner protocols) or GE SPGR sequence with approximately 1 mm³ resolution (although a variety of quality data sets can be processed with additional manual intervention). Thickness should not exceed 1.5 mm³ (~1mm³ is ideal). FreeSurfer provides the users two different tools to analyze and modify reconstructed images.

TkMedit is the main volume viewer and editor for FreeSurfer. It can be used to view volumes, overlay surfaces onto 2D, edit reconstruction defects, view functional overlays and time courses, view segmentations, and draw or edit labels.

TkSurfer allows visualization and navigation of cortical surface data. TkSurfer can also display functional or curvature data. The color sections of the original clip, white matters, pial, and tissues are shown in Fig. 3 to Fig. 6, respectively. The 3D model reconstruction of the left and right hemisphere highlighting the cortical thickness overlay is shown in Fig. 7 and Fig. 8, respectively.

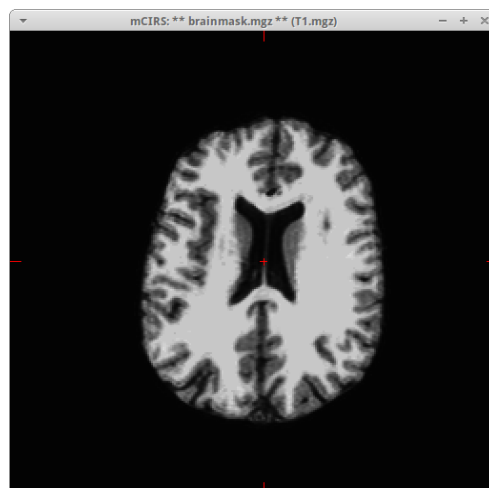


Fig. 3. Original anatomical data.

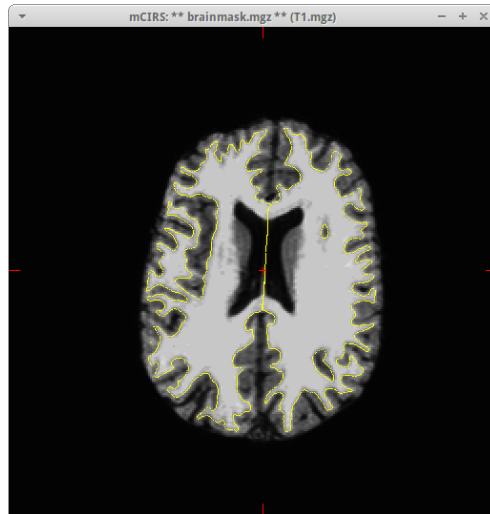


Fig. 4. White matter (in yellow).

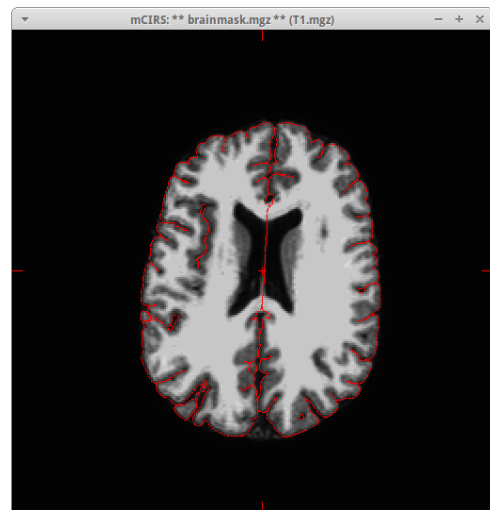


Fig. 5. Pial (in red).

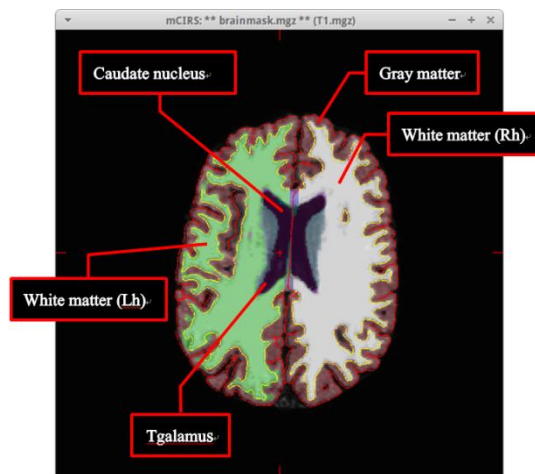


Fig. 6. Brain tissue distribution.

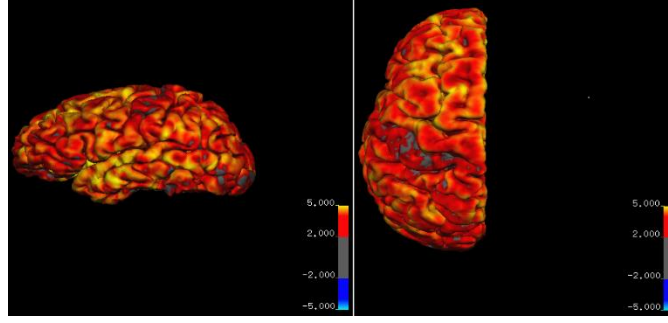


Fig. 7. 3D reconstruction of the left hemisphere plus cortical thickness overlay. The color scale represents the brain thickness in that specific point.

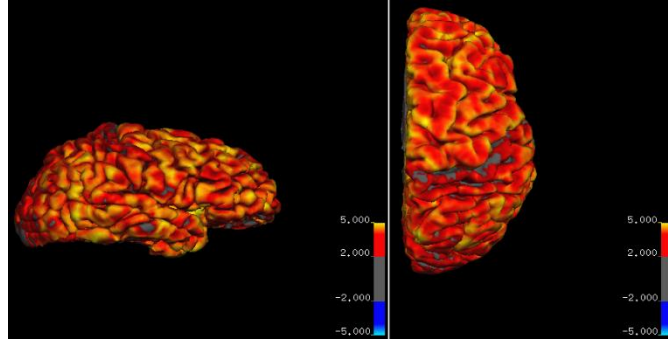


Fig. 8. 3D reconstruction of the right hemisphere and cortical thickness overlay. The color scale represents the brain thickness in that specific point.

3.2 Heat Kernel Smoothing

In order to enhance the signal-to-noise ratio we apply Gaussian kernel smoothing [11-14]. However, since the weights of the Gaussian kernel smoothing are determined by the Euclidean distance, it was decided to use the geodesic distance which works better in these cases. The difference between the two distances is shown in Fig. 9. The manifold smoothed data construct both a curve along the geodesic and the isotropic kernel. The heat kernel smoothing is a kernel with isotropic heat transfer and diffusion formula [11-14].

Consider the following random model of the cortical thickness on manifold $\partial\Omega$ [11-14]:

$$Y(p) = \theta(p) + \varepsilon(p), p \in \partial\Omega, \quad (1)$$

where $Y(p)$ is the thickness measurement, $\theta(p)$ is the true unknown thickness, $\varepsilon(p)$ is Gaussian noise with mean 0 and variance 0.2^2 . $\partial\Omega$ is assumed to be a 2D Riemannian manifold. Consider the positive definite kernel $K(p,q)$ of the form:

$$K_\sigma(p, q) = \sum_{i=0}^{\infty} e^{-\lambda_i \sigma} \sum_{m=-l}^{m=l} Y_{lm}(p) Y_{lm}(q). \quad (2)$$

where the ordered eigenvalues, $\lambda_{00} \geq \lambda_{1m1} \geq \lambda_{2m2} \dots \geq 0$, satisfy:

$$\int_{S^2} K(p, k) Y_{lm}(q) d\mu(q) = \lambda_{lm} Y_{lm}(p). \quad (3)$$

This is a special case of the Mercer's theorem. Without the loss of generality, we assume the kernel is normalized as follows:

$$\int_{S^2} K(p, k) d\mu(q) = 1. \quad (4)$$

The smooth functional estimation h of measurement f is searched in h_k that minimizes the integral of the weighted square distance between f and h :

$$\sum_{l=0}^k \sum_{m=-l}^l \lambda_{lm} f_{lm} Y_{lm} = \arg \min_{h \in h_k} \int_{S^2} \int_{S^2} K(p, k) |f(q) - h(p)|^2 d\mu(p) d\mu(q). \quad (5)$$

Kernel smoothing is defined as the integral convolution:

$$K * f(p) = \int_{S^2} f(q) k(p, q) d\mu(q) = \sum_{l=0}^{\infty} \sum_{m=-l}^l \lambda_{lm} \langle f, Y_{lm} \rangle Y_{lm}(p). \quad (6)$$

The flowchart of heat kernel smoothing method is shown in Fig. 10. Let the n vertex of polygon sphere \mathbf{S} be $\mathbf{p}_1, \dots, \mathbf{p}_n$. The neighborhood set of vertex is calculated, followed by the average weights $\tilde{\mathbf{W}}_\sigma$ and $\mathbf{Z}(\mathbf{p}_i)$, and then \mathbf{Y} is updated. The process is repeated for the preset iterations k . The effectiveness of the method is verified by comparing the real data with 20, 100, and 200 iterations, with simulated data with 20, 200, and 5,000 iterations. Fig. 11 shows the heat kernel smoothing applied to the data for one participant using Matlab.

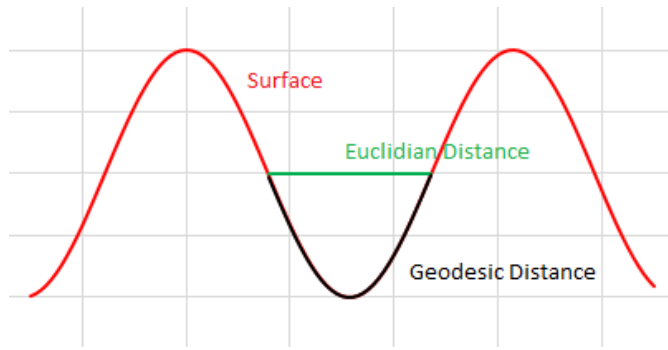


Fig. 9. Euclidian distance vs geodesic distance.

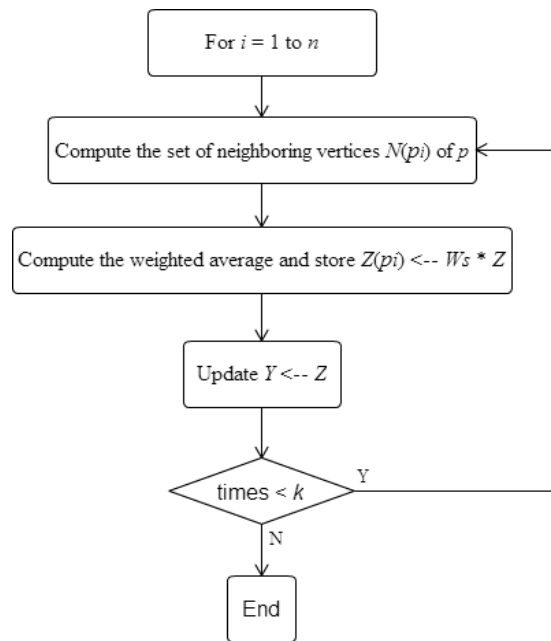


Fig. 10. Heat kernel smoothing flowchart.

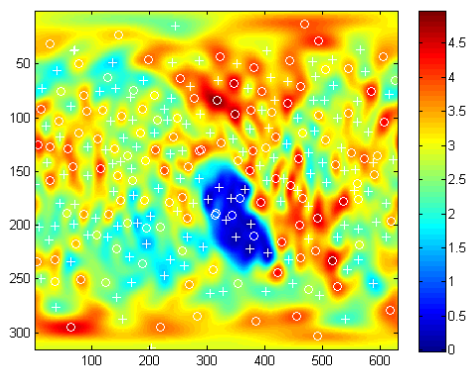


Fig. 11. Matlab plot of the heat kernel smoothing result applied to a participant with parameters $k = 30$ and $\sigma = 0.0005$.

3.3 Min-Max Diagram

A diagram proposed by Chung et al. [5] defines as Morse function, which is a function with its extremes independent while being non-degenerate. Let a Morse function be $\hat{\mu}$ and define a sublevel set as follows:

$$R(y) = \hat{\mu}^{-1}(-\infty, y), \quad (7)$$

The sublevel set must satisfy the condition of $\hat{\mu} \leq y$. When y increases from $-\infty$ the number of links in the set $R(y)$ sublevel vary whenever an extreme is surpassed. Assuming there are local minima g_1, g_2, \dots, g_m and local maxima h_1, h_2, \dots, h_n , since the extremes in the Morse function are assumed to be independent to each other, the local minima and maxima can be re-arranged in ascending order as follows:

$$g_1 < g_2 < \dots < g_m \quad (8)$$

$$h_1 < h_2 < \dots < h_n \quad (9)$$

At each local minimum there is a birth. When it meets a death from a local maximum both the birth and the death are fused to become a new sublevel in the sublevel set. This can be used to calculate the topological invariant of the sublevel set such as Euler characteristic and Betti numbers. The procedure to fuse the birth and the death is summarized as follows [5]:

Step 1: $H \leftarrow \{h_1, \dots, h_n\}$

Step 2: $i \leftarrow m$

Step 3: $h_i^* = \arg \min_{h_j \in H} \{h_j \mid h_j > g_i, h_j \sim g_i\}$

Step 4: If $h_i^* \neq \emptyset$, pair (g_i, h_j)

Step 5: $H \leftarrow H - h_i^*$

Step 6: If $i > 1$, $i \leftarrow i - 1$ and go to Step 3

H is the ordered set of local maxima and m is the number of local minima. In order to become a couple it chooses the smallest value that is larger than itself among the local maxima. If the candidate levels are not empty, the couple is generated. The couple is then removed from the ordered set H . The procedure continues until all the local minima have been coupled.

To illustrate how to couple both birth and death, we consider a curve plotted in Fig. 12. There are seven extremes labeled on the curve where the local minima are ordered by $C < A < E < G$ while the local maxima are

ordered $B < F < D$. Based on the coupling rule the nearest neighbor is chosen as couple. Consequently, (A,B) and (G,F) become sublevels. Although both local minima C and E are close to local maximum D E is closer to D that makes (E,D) a couple. Finally, each (birth, death) couple is plotted as the topological characteristic on the right hand side of Fig. 12.

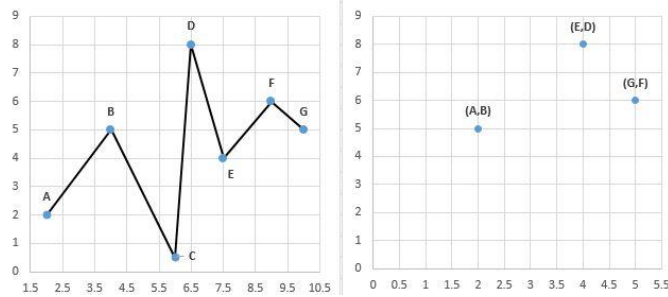


Fig. 12. Birth and death coupling. Left: a curve with seven extremes; right: topological characteristic.

4. THE FUZZY SYSTEM

Following Zadeh's work [15] we propose a fuzzy system which aims to indicate dementia risk on patients by analyzing their brain cortical thickness and hippocampus volume. The couple birth and death, and the normalized hippocampus volume are then the inputs of the system. While the first two inputs of our system are labeled Thin, Medium or Thick, the hippocampus is labeled Low, Medium or High as shown in Fig. 13, Fig. 14 and Fig. 15, respectively. To come up with birth and death inputs, given the persistence diagram we decided to cluster the points by fuzzy c-means where the maximum number of iterations is 1,000 and the stop criterion ϵ is 10^{-5} . The control and MCI participants were used as a training set to construct the inputs. Suppose three clusters are considered. The resulting centroids of our system are (2.2875, 3.4631), (2.5109, 4.0327) and (2.0200, 2.8125). Successively, we project these onto the x and y axis in order to design the input membership functions. The procedure is summarized in Fig. 16 while Fig. 17 shows the output membership functions. The hippocampus membership functions are constructed by ordering the volumes and taking the highest, medium and lowest. The output of the system is the risk of contracting dementia, labeled as Low, Medium or High and it comes from the 9 partitioned areas. The fuzzy rules base is composed by 27 different rules that are given in Table 1 and the partitioning is shown in Fig. 18. For each of the areas we calculate the ratio of MCI couples and we take the result of Thin – Thin, Medium – Medium and Thick – Thick to design the output membership functions. The ordered areas distributions are shown in Table 2.

Table 1. Proposed fuzzy rule base.

Rule No.	Birth	Death	Hippocampus	Output
R1	Thin	Thin	Low	High
R2	Thin	Thin	Medium	High
R3	Thin	Thin	High	High
R4	Thin	Medium	Low	High
R5	Thin	Medium	Medium	High
R6	Thin	Medium	High	High
R7	Thin	Thick	Low	Medium
R8	Thin	Thick	Medium	Medium
R9	Thin	Thick	High	Medium
R10	Medium	Thin	Low	High
R11	Medium	Thin	Medium	Medium
R12	Medium	Thin	High	Medium
R13	Medium	Medium	Low	Medium
R14	Medium	Medium	Medium	Medium
R15	Medium	Medium	High	Medium
R16	Medium	Thick	Low	Medium
R17	Medium	Thick	Medium	Medium
R18	Medium	Thick	High	Low
R19	Thick	Thin	Low	Low
R20	Thick	Thin	Medium	Low
R21	Thick	Thin	High	Low
R22	Thick	Medium	Low	Low
R23	Thick	Medium	Medium	Low
R24	Thick	Medium	High	Low
R25	Thick	Thick	Low	Low
R26	Thick	Thick	Medium	Low
R27	Thick	Thick	High	Low

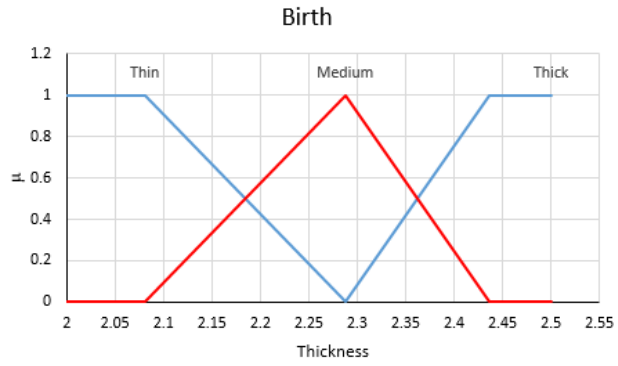


Fig. 13. Birth membership functions.

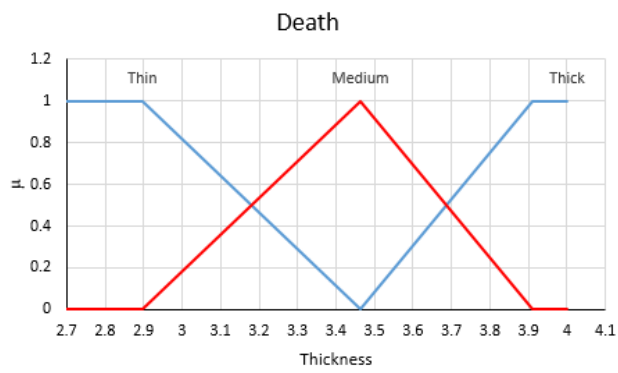


Fig. 14. Death membership functions.

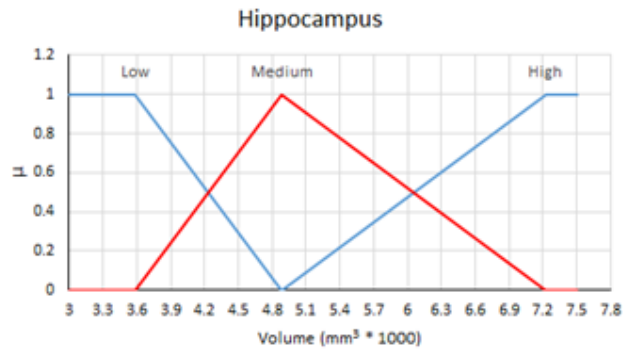


Fig. 15. Hippocampus volume membership functions.

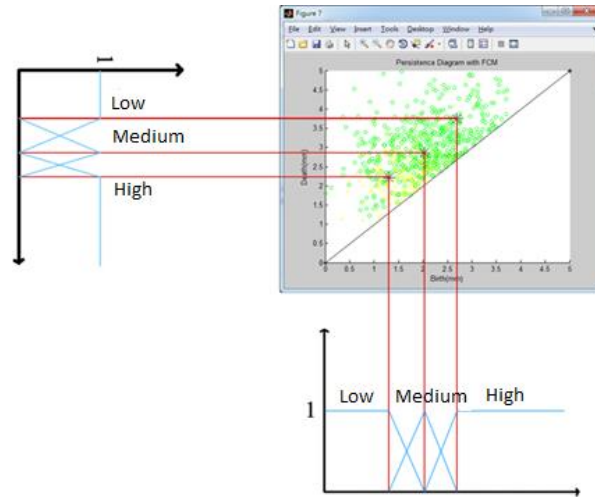


Fig. 16. Projection of the centroids with consequent input membership function design.

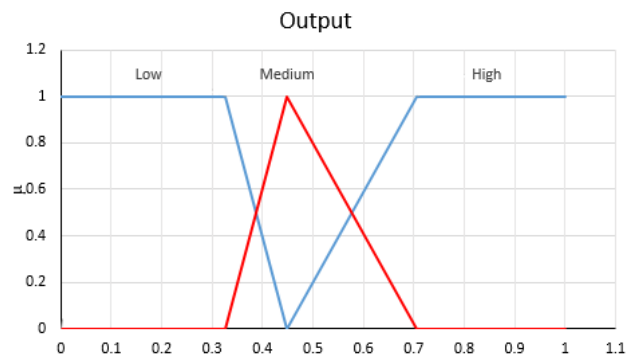


Fig. 17. Output membership functions.

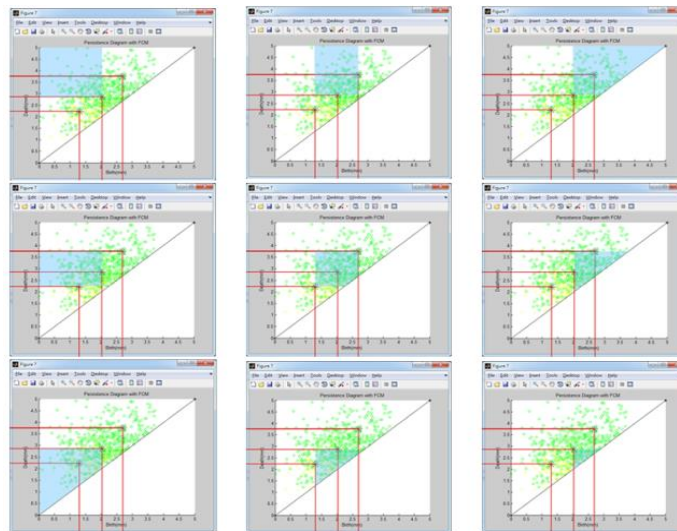


Fig. 18. Nine partitioned areas.

Table 2. Topological characteristic of the nine areas.

Thin-Thin	MCI	150	0.77720
	Control	43	
Thin-Medium	MCI	108	0.65454
	Control	57	
Thin-Thick	MCI	56	0.51852
	Control	52	
Medium-Thin	MCI	180	0.50562
	Control	176	
Medium-Medium	MCI	144	0.44037
	Control	183	
Medium-Thick	MCI	53	0.36552
	Control	92	
Thick-Thin	MCI	166	0.46239
	Control	193	
Thick-Medium	MCI	150	0.39894
	Control	226	
Thick-Thick	MCI	65	0.32020
	Control	138	

5. SIMULATION RESULTS AND ANALYSIS

5.1 Hardware and Patients' Results

The software was run on a laptop running the Xubuntu (<http://xubuntu.org/>) Linux distribution. The laptop was installed with an Intel Core i5 processor with 3MB L3 cache, 2GB of RAM and a 640GB hard-disk.

The reconstruction of a single 3D brain model requires up to 18 hours per patient while the overall size of the files is around 300-350MB. To analyze a patient is simple. We first calculate a set of centroids among subjects' birth-death couples and project the result onto the two input axes to infer membership degrees. The same is done by fuzzifying the normalized hippocampus volume to its corresponding membership functions. Then, the firing strength for each rule is calculated and defuzzified by center of gravity. More difficult is to find a specific range where the SCZ patients fall, due to the necessity for more examples and the nature of schizophrenia. Generally, they interfere with both control and suspicious exemplars, which is why we consider them either false positives or false negatives.

The system can also analyze a single brain hemisphere using the same fuzzy model. One of the reasons is that the output risk is generally close to the average of the two hemispheres taken separately (the hippocampus volume refers only to one of them according to the hemisphere). However, there are some patients with a low risk on one hemisphere and high on the other. Such cases are not uncovered when analyzing the entire brain. Moreover, we also noticed that AAMI and MCI patients generally show a thinner cortex on the left hemisphere compared to the right.

5.2 Comparing the Two Fuzzy Systems

An early prototype of our system took only into consideration inputs related to the cortical thickness, birth and death from the min-max diagram [7]. The system showed a good output response but failed to recognize some of the patients. By adding the hippocampus in the analysis, we have now a new system with a higher accuracy which does not fail to recognize control and MCI/AAMI subjects, as shown in Table 3 where we present 14 subjects with their own information and the output of the fuzzy systems, M1 (fuzzy output without hippocampus) and M2 (fuzzy output with hippocampus).

The two systems were also compared according to accuracy, balanced accuracy, sensitivity and specificity. Accuracy is the amount of true results among the subjects, while balanced accuracy is the arithmetic mean of sensitivity and specificity, which helps in avoiding inflated performance estimates on imbalanced data. Sensitivity and specificity of a quantitative test are dependent on the cut-off value above or below which the test is positive [16]. Specifically, the sensitivity refers to the ability of the test to correctly identify patients with disease. On the other hand, the specificity refers to the ability of the test to correctly identify patients without the disease. Positive predictive value (PPV) tests how likely a patient has the disease given that the test result is positive and negative predictive value (NPV) tests how likely the patient does not have the disease given that the test result is negative.

The following terms are fundamental to understanding the utility of clinical tests [9]:

1) True positive (TP)

The patient has the disease and the test is positive.

2) False positive (FP)

The patient does not have the disease but the test is positive.

3) True negative (TN)

The patient does not have the disease and the test is negative.

4) False negative (FN)

The patient has the disease but the test is negative.

Thus, the following equations are now easy to understand:

$$Accuracy = \frac{True\ positives + True\ negatives}{Participants\ (TP + FP + TN + FN)}. \quad (10)$$

$$Sensitivity = \frac{True\ positives}{True\ positives + False\ negatives}. \quad (11)$$

$$Specificity = \frac{True\ negatives}{True\ negatives + False\ positives}. \quad (12)$$

$$Positive\ Predictive\ Value\ (PPV) = \frac{True\ positives}{True\ positives + False\ positives}. \quad (13)$$

$$Negative\ Predictive\ Value\ (NPV) = \frac{True\ negatives}{True\ negatives + False\ negatives}. \quad (14)$$

$$Balanced\ Accuracy = \frac{Sensitivity + Specificity}{2}. \quad (15)$$

Sensitivity and specificity was calculated for 10 patients as shown in Table 4 in addition to another four patients that were used for the blind test. These four patients are correctly analyzed by the new system while the M1 system fails in recognizing subject four. As can be seen, there is a general improvement for the M2 system. At the present, excluding the SCZ, the system achieves a 100% accuracy on recognizing controls and MCI/AAMI patients. Finally the patients' coordinates in 2D (birth and death) and 3D (birth, death and hippocampus volume) graphs are shown in Fig. 19 and Fig. 20, respectively. These graphs show that the distribution of MCI/AAMI and healthy patients are well-separated while the SCZ subjects' coordinates mingle with others over the graph surface that results in a difficult analysis for these patients.

Table 3. Inference results from the two fuzzy models.

ID	Gender	Age	Symptom	M1	M2	Class	
						M1	M2
1	F	75	MCI	0.6527	0.6527	TP	TP
2	M	86	MCI	0.6901	0.7137	TP	TP

3	F	75	MCI	0.4122	0.6299	FN	TP
4	F	72	MCI	0.3484	0.6413	FN	TP
5	F	26	SCZ	0.5618	0.5962	FP	FP
6	F	38	SCZ	0.2154	0.2154	FN	FN
7	M	21	SCZ	0.2195	0.2195	FN	FN
8	F	67	AAMI	0.6706	0.6826	TP	TP
9	M	63	AAMI	0.6556	0.6556	TP	TP
10	F	44	Healthy	0.2827	0.2894	TN	TN
11	M	43	Healthy	0.2421	0.2421	TN	TN
12	F	19	Healthy	0.2069	0.2115	TN	TN
13	F	19	Healthy	0.2069	0.2069	TN	TN
14	M	26	Healthy	0.2387	0.2441	TN	TN

Table 4. Comparison of M1 and M2 systems.

Classification Trials		
	M1	M2
TN	5	5
TP	4	6
FP	1	1
FN	4	2
Total	14	14
Accuracy	64.3%	78.6%
Balanced	66.7%	79.2%
Accuracy		
Sensitivity	50.0%	75.0%
Specificity	83.3%	83.3%
PPV	80.0%	85.7%
NPV	55.6%	71.4%

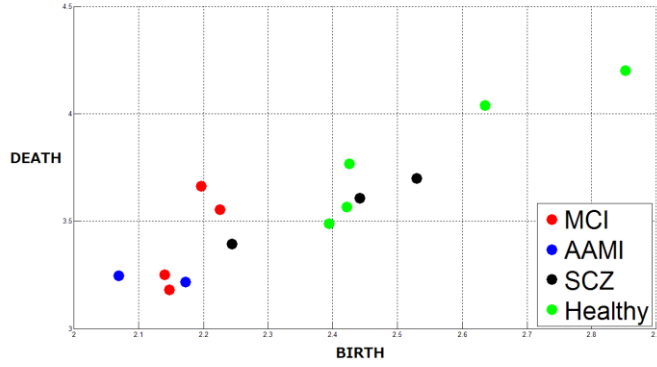


Fig. 19. X-axis refers to birth and Y-axis refers to death. Red, blue, black and green refers to MCI, AAMI, SCZ and control patients, respectively.

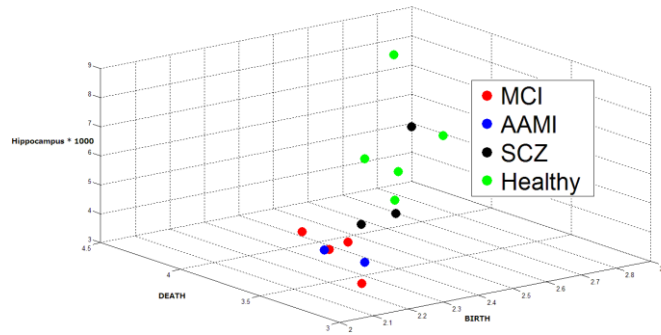


Fig. 20. X-axis refers to birth, Y-axis refers to death and Z-axis refers to the hippocampus volume. Red, blue, black and green refers to MCI, AAMI, SCZ and control subjects, respectively.

5.3 Attributes Analysis

Among the AD and MCI cases the literature also reports that ventricular enlargement may be an objective and sensitive measure of neuropathological change associated with mild cognitive impairment and Alzheimer's disease [17]. There are four ventricles in the brain: the so-called lateral ventricles, left and right, and the third and fourth ventricles. Freesurfer, in the aseg.stats file provides volume measures for all of them, this is why we apply the information gain on the subjects to select important features. To recall the main concept beneath the information gain, let's consider a table S containing s_i tuples class c_i for $i=\{1,\dots,m\}$. The information represents the expected amount of information required to classify any arbitrary tuples, and it is defined as follows:

$$I(s_1, s_2, \dots, s_m) = - \sum_{i=1}^m \frac{s_i}{S} \log_2 \frac{s_i}{S}. \quad (16)$$

Then, we define the entropy of the attribute A with range of values $\{a_1, a_2, \dots, a_v\}$:

$$E(A) = - \sum_{j=1}^v \frac{s1j + \dots + smj}{S} I(s1j, \dots, smj). \quad (17)$$

The information gained by branching on attribute A is defined as follows:

$$Gain(A) = I(s1, s2, \dots, sm) - E(A). \quad (18)$$

We aim to investigate which of the attributes (birth, death, normalized hippocampus volume, normalized first ventricle volume, normalized second ventricle volume, normalized third ventricle volume, normalized fourth ventricle volume) provides the highest amount of information. Table 5 shows the list of subjects taken in examination with their brain volumes measures. The ‘‘S?’’ column reflects the output of our system. ‘‘Y’’ means output > 0.6 while ‘‘N’’ means ≤ 0.6 . The first step is to apply the generalization which consists in joining the values in ranges as shown in Table 6. At this point we calculated the information gain for every attribute and Table 7 shows the ordered gains. The second ventricle, according to our generalization, carries a higher amount of information than death and hippocampus, which means that it is an important attribute in terms of characterization of the patient. The listed order, however, reflected our good choice in terms of input of the fuzzy system since our inputs were in the top 4 of the most important attributes.

Table 5. Information gain.

ID	Birth	Death	HN	1VN	2VN	3VN	4VN	S?
A1	2.1399	3.2506	0.0049	0.0087	0.0096	0.0014	0.0016	Y
A2	2.1473	3.1794	0.0037	0.0145	0.0116	0.0008	0.0017	Y
A3	2.2251	3.5540	0.0040	0.0211	0.0209	0.0021	0.0015	Y
A4	2.2440	3.3936	0.0051	0.0071	0.0069	0.0005	0.0006	Y
A5	2.4417	3.6072	0.0051	0.0127	0.0207	0.0009	0.0012	N
A6	2.5294	3.6990	0.0072	0.0038	0.0031	0.0007	0.0016	N
A7	2.1721	3.2175	0.0043	0.0103	0.0115	0.0013	0.0011	Y
A8	2.0690	3.2449	0.0052	0.0062	0.0070	0.0008	0.0013	Y
A9	2.3936	3.4873	0.0064	0.0056	0.0058	0.0005	0.0007	N
A10	2.4212	3.5670	0.0050	0.0139	0.0125	0.0004	0.0009	N

Table 6. Generalized information gain.

ID	Birth	Death	HN	1VN	2VN	3DN	4VN	S?
----	-------	-------	----	-----	-----	-----	-----	----

A1	≤ 2.15	3.25... 3.50	medium	medium	medium	high	high	Y
A2	≤ 2.15	≤ 3.25	low	high	medium	medium	high	Y
A3	2.15... 2.25	≥ 3.5	low	high	high	high	medium	Y
A4	2.15... 2.25	3.25... 3.50	high	medium	low	low	low	Y
A5	≥ 2.25	≥ 3.5	medium	medium	high	medium	medium	N
A6	≥ 2.25	≥ 3.5	high	low	low	medium	high	N
A7	2.15... 2.25	≤ 3.25	low	medium	medium	high	medium	Y
A8	≤ 2.15	≤ 3.25	medium	low	medium	medium	medium	Y
A9	≥ 2.25	3.25... 3.50	high	low	low	low	low	N
A10	≥ 2.25	≥ 3.5	high	high	high	low	low	N

Table 7. Ordered gains.

Gains in order	
Gain (birth)	0.9709506
Gain (2 nd ventricle)	0.4199731
Gain (death)	0.3709506
Gain (hippocampus)	0.2954618
Gain (3 rd ventricle)	0.2954618
Gain (1 st ventricle)	0.0954618
Gain (4 th ventricle)	0.0954618

6. CONCLUSIONS

Alzheimer's disease constitutes one of the major problems in modern society where it impacts a high percentage in the elderly population. In Taiwan, statistics from the Ministry of Health and Welfare, Taiwan, estimated that Taiwan will become an aged society in 2018 [18]. To systematically assess AD at an early stage, a fuzzy system is proposed that infers reliable biomarkers in assisting physician's clinical diagnosis. The possibility to analyze the hippocampus volumes as the third input of the fuzzy systems, we can discriminate between control and AAMI/MCI subjects. Moreover, adding hippocampus volume as the third input to the proposed fuzzy systems reduced the number of false positive among the analyzed participants. Experiment results verified that the proposed fuzzy models were effective in discriminating the dementia risk of control to AAMI/MCI subjects.

Future work involves using the brain ventricles in a more comprehensive study to delineate the most noticeable changes in brain structure. For example, preliminary data show the second ventricle carries a high amount of information may be an important factor in the model. Besides, reducing the time complexity to obtain the dementia risk of a subject is also worth addressing. Finally, this study was limited the small sample size. Future studies should attempt to include larger samples.

ACKNOWLEDGMENTS

This work was supported in part by the Ministry of Science and Technology, Taiwan under Grants MOST103-2221-E-027-122-MY2 and by a joint project between the National Taipei University of Technology and Mackay Memorial Hospital under Grants NTUT-MMH-105-04 and NTUT-MMH-104-03.

REFERENCES

- [1] Alzheimer's Disease International (ADI), <http://www.alz.co.uk/>.
- [2] B.C. Dickerson and D.A. Wolk, "MRI cortical thickness biomarker predicts AD-like CSF and cognitive decline in normal adults," *Neurology*, vol. 78, no. 2, pp.84-90, Jan. 2012.
- [3] http://www.hbmsp.sipa.gov.tw:9090/itri/tw/images/NewsList1000913_06.htm.
- [4] M.K. Chung, S.M. Robbins, K.M. Dalton, R.J. Davidson, A.L. Alexander and A.C. Evans, "Cortical thickness analysis in autism with heat kernel smoothing," *Neuroimage*, vol. 25, no. 4, pp.1256-1265, May 2005.
- [5] M.K. Chung, V. Singh, P.T. Kim, K.M. Dalton and R.J. Davidson, "Topological characterization of signal in brain images using min-max diagrams," in *Proc. of Int. Conf. on Medical Image Computing and Computer Assisted Intervention*, London, UK, part II, LNCS 5762, pp.158-166, 2009.
- [6] N. Schuff, "MRI of hippocampal volume loss in early Alzheimer's disease in relation to ApoE genotype and biomarkers," *Brain*, vol. 132, Pt. 4, pp.1067-77, Apr. 2009.
- [7] Y.-P. Huang and S. Zaza, "A fuzzy approach to evaluating the risk of dementia by analyzing the cortical thickness from MRI," in *Proc. of IEEE Int. Conf. on System Science and Engineering*, Shanghai, China, pp.88-93, July 2014.
- [8] A.M. Dale, B. Fischl and M.I. Sereno, "Cortical surface-based analysis I: segmentation and surface reconstruction," *Neuroimage*, vol. 9, no. 2, pp.179-194, 1999.

- [9] P. Melillo, N.D. Luca, M. Bracale and L. Pecchia, "Classification tree for risk assessment in patients suffering from congestive heart failure via long-term heart rate variability," *IEEE Journal of Biomedical and Health Informatics*, vol. 17, no. 3, pp.727-733, May 2013.
- [10] B. Fischl, M.I. Sereno and A.M. Dale, "Cortical surface-based analysis II: inflation, flattening, and a surface-based coordinate system," *Neuroimage*, vol. 9, no. 2, pp.195-207, 1999.
- [11] M.K. Chung, S. Robbins and A.C. Evans, "Unified statistical approach to cortical thickness analysis," *Information Processing in Medical Imaging*, LNCS 3565, pp.627-638, 2005.
- [12] M.K. Chung, *Heat kernel smoothing and its application to cortical manifolds*, Department of Statistics, University of Wisconsin-Madison, Technical Report 1090, 2004.
- [13] M.K. Chung, K.M. Dalton and R.J. Davidson, "Tensor-based cortical surface morphometry via weighted spherical harmonic representation," *IEEE Trans. on Medical Imaging*, vol. 27, no. 8, pp.1143-1151, Aug. 2008.
- [14] M.K. Chung, K.M. Dalton, L. Shen, A.C. Evans and R.J. Davidson, "Weighted Fourier series representation and its application to quantifying the amount of gray matter," *IEEE Trans. on Medical Imaging*, vol. 26, no. 4, pp.556-581, Apr. 2007.
- [15] L.A. Zadeh, "Fuzzy sets," *Information and Control*, vol. 8, no. 3, pp.338-353, Jun. 1965.
- [16] A.G. Lalkhen and A. McCluskey, "Clinical tests: sensitivity and specificity," *Continuing Education in Anaesthesia, Critical Care & Pain*, vol. 8, issue 6, pp.221-223, 2008.
- [17] L.G. Apostolova, A.E. Green, S. Babakchian, K.S. Hwang, Y.Y. Chou, A.W. Toga and P.M. Thompson, "Hippocampal atrophy and ventricular enlargement in normal aging, mild cognitive impairment (MCI), and Alzheimer Disease," *Alzheimer Disease and Associated Disorders*, vol. 26, no. 1, pp.17-27, Jan.-Mar. 2012.
- [18] <http://health99.hpa.gov.tw/Default.aspx>